



Sharif University of Technology
Scientia Iranica
Transactions A: Civil Engineering
www.scientiairanica.com



Experimental investigation of square RC column strengthened with near surface mounted GFRP bars subjected to axial and cyclic lateral loads

N. Dayhim^{a,*}, A. Nicknam^a, M.A. Barkhordari^a, A. Hosseini^b and S. Mehdizad^c

a. Department of Civil Engineering, Iran University of Science and Technology, Tehran, P.O. Box 16765-163, Iran.

b. Department of Civil Engineering, Tehran University, Tehran, P.O. Box 11365-4563, Iran.

c. Department of Civil Engineering, Sharif University of Technology, Tehran, P.O. Box 11155-9313, Iran.

Received 30 June 2012; received in revised form 3 December 2012; accepted 26 January 2013

KEYWORDS

Cyclic lateral load;
GFRP bar;
Near-surface mounted
technique;
GFRP wrap;
Ductility;
Flexural
strengthening.

Abstract. This article is intended to highlight the effectiveness of longitudinal Glass Fiber Reinforced Polymer (GFRP) bars in combination with GFRP sheets on the flexural capacity of Reinforced Concrete (RC) columns. Seven half-scale RC columns including five strengthened and two control unstrengthened specimens were experimentally tested under axial and cyclic lateral loads. The strengthened columns with two different longitudinal GFRP bar ratios were tested under three different axial load levels. The flexural strength and ductility parameters of the specimens were calculated by obtaining their deformations and measuring the loads from load cells. The experimental results indicate significant increase in the flexural strength of the RC specimens. The results of this study can be reliably utilized to enhance the flexural strength of RC columns in the regions with high seismicity.

© 2013 Sharif University of Technology. All rights reserved.

1. Introduction

Fiber Reinforced Polymer (FRP) composite jacketing system is an efficient technology for upgrading the shear strength, flexural ductility and axial resistance of Reinforced Concrete (RC) columns. FRP jacketing system provides lateral confinement which leads to an increase in concrete compressive strength, as well as ultimate strain of concrete [1-5]. It also improves the seismic resistance and energy absorption of RC columns [4]. This confinement effect prevents the buckling of longitudinal steel bars, restrains the lateral

concrete expansion, and causes delay in the spalling of cover concrete. Over the last decade, a number of researchers have demonstrated the effectiveness of FRP composites in improving the seismic performance and capacity of structures [1-7]. Fiber reinforced polymers also improve the shear strength and ductility of beam-column joints. The experimental and analytical results of external retrofitting techniques, concerning the rehabilitation of deficient RC joints with FRP composites, confirm the capability of these methods in improving the strength capacity of RC joints, relocating the plastic hinges away from the column face and preventing the joint core brittle failure mode [8-10].

Traditionally, the flexural capacity of RC members has been modified by FRP sheets [1-3]. In this technique, the vertical FRP sheets parallel to the longitudinal steel reinforcements, anchored by steel an-

*. Corresponding author. Tel.: +98 21 77240399;

Fax: +98 21 77240398

E-mail addresses: nima_dayhim@yahoo.com (N. Dayhim), a_nicknam@iust.ac.ir (A. Nicknam), barkhordar@iust.ac.ir, (M.A. Barkhordari), hosseiniaby@ut.ac.ir (A. Hosseini), shahabmehdizad@yahoo.com (S. Mehdizad)

chorage, are utilized to enhance the flexural capacity of RC columns. In this strengthening method, FRP sheets should be anchored to the adjacent members. Such anchorages may cause premature rupture of FRP sheets due to the stress concentration in anchorage zone [3]. The use of Near-Surface Mounted (NSM) FRP bars is an alternative strengthening approach to enhance the flexural strength of RC structures. This method was developed in Europe in 1950s. In 1948, an RC bridge deck in Sweden was upgraded by steel cages. This technique was accomplished by inserting steel reinforcement bars into the grooves, which were made in concrete surfaces and were filled with cement mortar [11]. Currently, FRP bars with epoxy paste are widely used in retrofitting RC structures [12–17].

The advantages of Near-Surface Mounted FRP bars in comparison with externally bonded FRP composites in retrofitting RC structures, to increase the flexural capacity of RC beams, have been successfully shown by De Lorenzis and Nanni, Yast et al., Barros et al., Carolin et al. and El-Hacha and Rizkalla [15–21]. An important advantage of NSM-FRP bars is the possibility of anchoring reinforcement into the adjacent members, as shown by Nanni et al. [22]. This technique becomes particularly attractive for the flexural strengthening in the negative moment regions of slabs and girders, where externally bonded FRP composites can be subjected to severe damages due to mechanical and environmental conditions [22]. This technique does not need any surface preparation work, and can be accomplished with minimal installation time after cutting the grooves, as compared with externally bonded FRP composites, because the use of primer and putty is normally not necessary [23]. Barros et al. [19] successfully used NSM composite system to improve the seismic performance of RC columns. Recently, Bournas and Triantafillou [24] have experimentally demonstrated that the flexural resistance and ductility of RC columns under seismic loading can be enhanced by NSM-FRP bars in combination with CFRP wraps. In full scale tests carried out by Alkhrdaji et al. [23], it was concluded that using Glass Fiber Reinforced Polymer (GFRP) bars with higher strain and lower modulus, compared to Carbon Fiber Reinforced Polymer (CFRP) bars, leads to higher structural ductility in the flexural strengthening of RC columns. Additional to the above mentioned studies, still more experimental research work is needed to assess the upgrading levels of the flexural capacity of RC columns by means of longitudinal GFRP bars.

The use of Near-Surface Mounted (NSM) GFRP bars in combination with GFRP sheets to increase the structural ductility, while keeping the stiffness constant, ends up with considerable enhancement in the flexural strength of RC structures. This idea has been the main motivation in this study. This article

presents the results of experimental investigations on the flexural performance and capacity of RC columns, reinforced with longitudinal GFRP bars in combination with GFRP wraps by means of Near-Surface Mounted technique under axial and cyclic lateral loads.

2. Experimental program

2.1. Test specimens

A total of seven square reinforced concrete columns were tested under cyclic lateral load, while simultaneously being subjected to constant axial load throughout the test. Each specimen consists of a 250 mm wide and 900 mm long column which has been integrally cast with a 300 mm × 400 mm × 850 mm stub. The stub represents a discontinuity such as a beam-column joint or a footing. The specimens were reinforced with six longitudinal steel bars with diameter of 12 mm ($\rho_l = 1.08\%$, where ρ_l is the ratio of longitudinal steel reinforcement area to gross area of concrete), and were confined with transverse steel ties with diameter of 8 mm spaced at 100 mm ($\rho_s = 1.4\%$, where ρ_s is the volumetric ratio of transverse steel reinforcement to core concrete). The longitudinal bars in the columns completely extended into the stub were bent with a 90° hook, and confined with steel transverse ties spaced at 50 mm. The corners of the strengthened columns were beveled by placing triangular wood sections inside the forms during the cast. All of the specimens were cast in a horizontal position. The details of the test specimens are shown in Figure 1.

The test specimens have been given descriptive names. Each column is identified with an acronym,

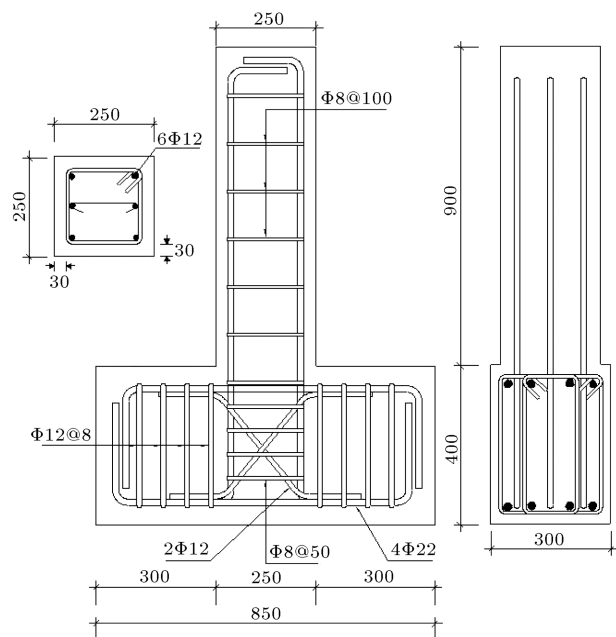


Figure 1. Reinforcing details of the specimens (all dimensions are in mm).

where C denotes control and R indicates retrofitted specimen. Seven half-scale RC columns consisted of two unstrengthened specimens (named C_1 and C_2), and five strengthened specimens (R_1 to R_5), are investigated to study the influence of NSM-GFRP bar reinforcement ratio, ρ_{NSM} , in combination with GFRP wraps on their flexural performance and capacity. Table 1 shows the details of the test specimens. In the unstrengthened specimens, the specimen C_1 was tested under axial and cyclic lateral loads, whereas the specimen C_2 was tested only under cyclic lateral load. In the strengthened specimens, the specimen R_1 was strengthened with three layers of GFRP sheets. The specimens R_2 to R_5 were strengthened with two different GFRP bar reinforcement ratios, $\rho_{NSM} = 0.5\%$ and 0.75% , mounted on two opposite sides. After the mounting process, these specimens were confined with three unidirectional GFRP sheets being wrapped in a continuous manner. These specimens were tested under three levels of axial loads and cyclic lateral loading. The specimens C_1 and R_2 were tested without axial load, whereas the specimens C_2 , R_1 , R_4 and R_5 were axially loaded at 438 kN ($0.2P_0$, where P_0 is the axial load of capacity of column) and the specimen R_3 was axially loaded at 219 kN ($0.1P_0$). The axial load was applied by a hydraulic jack, controlled by a load

cell. The axial load was manually kept constant during the cyclic lateral loading.

2.2. Material properties

The specimens were horizontally cast with four batches of concrete, using mixed normal-weight concrete with a slump of approximately 100 mm . Portland cement, natural sand and round river gravel with maximum nominal size of 12 mm were used for the mixture designed for target strength of 35 MPa . The strength of each RC specimen was obtained by averaging the values obtained from three standard cylinder tests (Table 1). The corners of the strengthened specimens were rounded to a radius of 25 mm . All of the specimens were tested around 60 days after curing under the laboratory conditions; the strengthening process, and the preparation of the specimens consist of test set-up and instrumentations before performing the tests.

The properties of longitudinal GFRP bars, GFRP composite sheets and epoxy system are shown in Table 2. Grade 400 steel was used for longitudinal and transverse steel bars. The epoxy system is comprised of two constituents, resin and hardener, mixed with 2:1 ratio. The epoxy system was hand-mixed, which requires a preparation time of at least 5 min .

Table 1. Details of test specimens.

Specimen	Longitudinal steel		Transverse steel		f'_c (MPa)	$\frac{P}{P_0}$	Strengthening regime	
	Diam. (mm)	ρ_l (%)	Diam. (mm)	ρ_s (%)			No. of longitudinal GFRP bars, ρ_{NSM} (%)	No. of layers of GFRP sheets
C_1	12	1.08(%)	8	1.4(%)	34.5	0	Na	Na
C_2	12	1.08(%)	8	1.4(%)	33.7	0.2	Na	Na
R_1	12	1.08(%)	8	1.4(%)	32.9	0.2	Na	3
R_2	12	1.08(%)	8	1.4(%)	36.1	0	4, (0.5)	3
R_3	12	1.08(%)	8	1.4(%)	34.7	0.1	4, (0.5)	3
R_4	12	1.08(%)	8	1.4(%)	38.7	0.2	4, (0.5)	3
R_5	12	1.08(%)	8	1.4(%)	36.5	0.2	6, (0.75)	3

Note: f'_c : Concrete compressive strength; P : Axial load on column; P_0 : Axial load of capacity of column, ($P_0 = 0.85f'_c(A_g - A_{st}) + f_{yt}A_{st}$); Na: not applicable.

Table 2. Mechanical properties of steel and composite reinforcements and epoxy system.

Material	Diameter (mm)	Elastic modulus (GPa)	Yield strength (MPa)	Tensile strength (MPa)	Ultimate strain ^a (%)
GFRP sheet	0.33	77	-	1694	2.2
Epoxy paste	-	10	-	60	-
GFRP bar	10	43	-	900	2.09
Steel bar	8; 12; 22	210	400	600	15

^a: Based on tension coupon test.

2.3. Strengthening procedure

In the strengthening process of the specimens in the first stage, the corners of the columns were rounded to 25 mm radius after the curing. The longitudinal grooves with 20 mm deep and 20 mm wide, parallel to longitudinal steel bars, were made on two opposite sides of the specimens and were cleaned by sand blasting. In the second stage, longitudinal GFRP bars were mounted in these longitudinal grooves. The specimens R_2 , R_3 and R_4 were strengthened with four GFRP bars, whereas the specimen R_5 was strengthened with six GFRP bars.

The mounting process was performed in four steps. In the first step, the drilled holes in the stub were filled with epoxy paste. In the second step, half of the grooves' depth was filled with epoxy. In the third step, GFRP bars were mounted, and the grooves were covered and smoothed with epoxy paste. Finally, the height of each strengthened specimen was entirely confined with three layers of GFRP sheets. GFRP bars were anchored with the embedment length of approximately 250 mm into the stub and were fixed in the drilled holes by epoxy paste.

To confine the specimens with GFRP sheets, a thin layer of epoxy was applied to the surfaces of the specimens, and a unidirectional GFRP sheet was then wrapped around the column. Subsequently, the second layer of epoxy paste was added to the surfaces of the first layer of GFRP wrap. This process was repeated until confining the columns with three layers of GFRP sheets. Finally, a layer of epoxy was applied to the third layer of GFRP sheet. The fibers in GFRP wraps were oriented at an angle of 90° with respect to the longitudinal axis of column. The third layer of GFRP sheet was extended by 100 mm to ensure the development of full composite strength. The wrapped columns were left at room temperature for at least 7 days before performing tests (Figure 2).

2.4. Test set-up and instrumentations

All of the specimens were tested under the condition that cyclic lateral displacements were progressively increased up to a large predefined inelastic deformation level, while being simultaneously subjected to axial load (see Figure 3). One vertical and two horizontal hydraulic jacks were utilized to apply axial and cyclic lateral loads, respectively. A vertical hydraulic jack with a capacity of 1000 kN was used to apply the axial load, measured by a load cell. In the beginning of each test, the axial load was applied to the specimens. Subsequently, the specimens were subjected to gradually increasing lateral displacement cycles through applying reversed cyclic lateral loads. The cyclic lateral loads were applied through 26 loading-reloading cycles, followed by the displacement protocol shown in Figure 4. The cyclic lateral load was applied

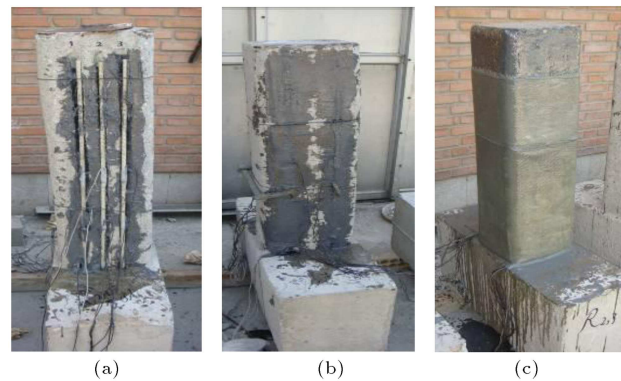


Figure 2. Adopted flexural strengthening in Near-Surface Mounted technique: a) Making grooves on two opposite sides of the columns, drilling holes at the base level of the columns for anchorage of GFRP bars, applying epoxy paste and installing 2 or 3 GFRP bars on each side; b) applying epoxy paste and leveling the surfaces; and c) applying three layers of GFRP wraps.

by two hydraulic jacks with a capacity of 500 kN. These hydraulic jacks were used to displace the top of the columns to achieve a predefined displacement level. The stubs of the specimens were fixed to the strong floor by eight high-strength rods, prestressed by 200 kN force to prevent the sliding and the probable overturning under large cyclic lateral loads.

A predefined lateral displacement of 825 mm from the stub was monitored by two horizontal Linear Variable Displacement Transducers (LVDTs). One horizontal LVDT was installed at the base level of the column to measure the sliding of the stub. Moreover, the curvature of the column was calculated by measuring the differences in the axial strains, using twelve LVDTs at the opposite sides of the columns, positioned at 30 mm, 130 mm, 230 mm, 330 mm and 430 mm from the stub (Figure 3). The longitudinal strains in steel and GFRP bars were measured with 60 mm long strain gages, installed at different locations (see Figure 5). Also, twelve 60 mm long strain gages were installed at different locations on the third layer of GFRP sheet to measure the lateral strain of GFRP wrap. The location of strain gages is shown in Figure 5.

3. Experimental results and discussions

3.1. Lateral load-drift ratio curves and ductility parameters

A number of ductility and deformability definitions are available in the literature [25–27]. In this article, the ductility parameters suggested by Khoury and Sheikh [27] are adopted to evaluate the performance of the test specimens. The failure of the column is defined in the post-peak behavior, where the column capacity drops to 80% of the peak load. It is desirable to define response indices to quantify the column

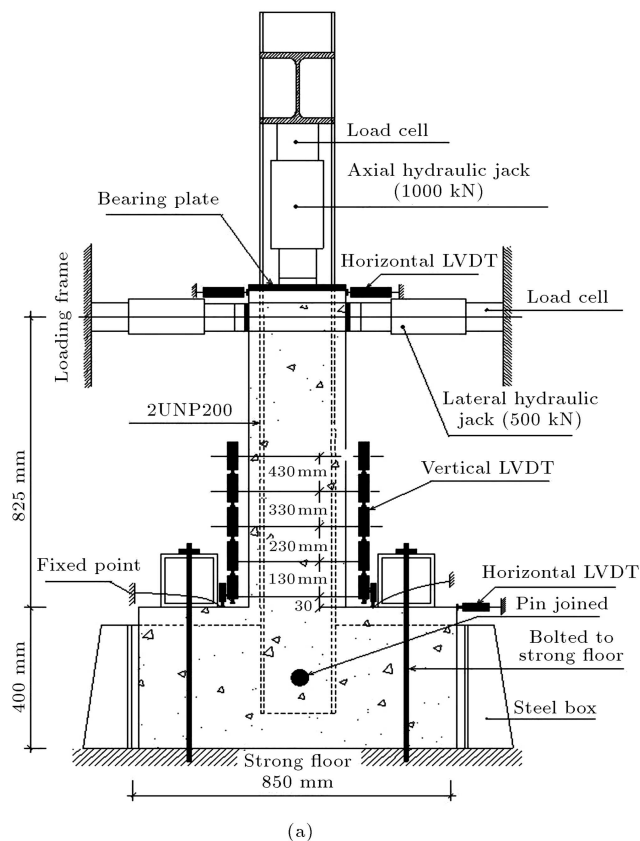


Figure 3. Test set-up; location of instrumentations (twelve vertical Linear Variable Displacement Transducers (LVDTs) and three horizontal LVDTs) (all dimensions are in mm): a) Details and dimensions; and b) photograph.

behavior. In seismic design, the inelastic deformation is generally quantified by the member ductility parameters. These parameters include displacement ductility, μ_{Δ} , cumulative ductility ratios, N_{Δ} , and work damage indicator, W . Figure 6 shows the definition of the member ductility parameters, μ_{Δ} , N_{Δ} , and W . The subscripts t and 80 are added to N_{Δ} and W , respectively, to indicate the value of each parameter up to the end of the test and until the end of the cycle in which the shear force is dropped to approximately 80 percent of the peak load. Ductility factors and cumulative ductility ratios describe the deformability

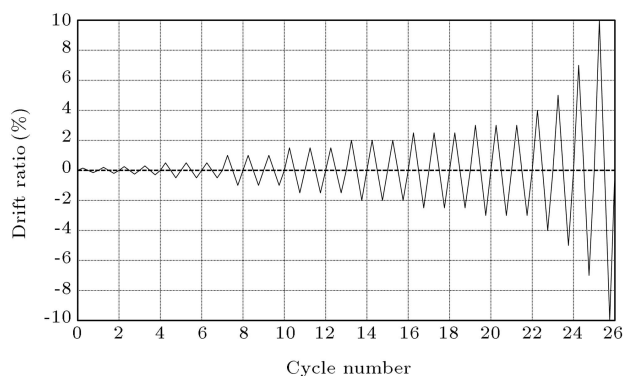


Figure 4. Loading procedure.

of the member, whereas damage indicators estimate the toughness of the member. The yield displacement, Δ_y , is calculated by extrapolating a straight line from the shear force-drift ratio coordinate at $0.75V_{\max}$ to the maximum shear force, V_{\max} . This procedure is shown in Figure 7. The yield displacement, Δ_y , used in the tests, is the average of the values obtained from two directions. The plots of the shear force versus drift ratio for the unstrengthened and strengthened specimens are shown in Figures 8 and 9, respectively. Moreover, these figures show the displacement ductility factor, μ_{Δ} , corresponding to twenty percent strength drop and the average of maximum lateral load in two opposite directions, V_{\max} . The related envelope curves for the shear force-drift ratio are shown in Figure 10.

Table 3 demonstrates the test results in terms of lateral load, corresponding to the initiation of yielding at steel bars, V_y , the yield displacement, Δ_y , the maximum lateral load, V_{\max} , the displacement ductility factor, μ_{Δ} , the cumulative ductility ratios, N_{Δ} , and the work damage indicator, W . The compressive strain at the extreme compression fiber, $\varepsilon_{c,\text{peak}}$, the strain in steel bar at tension fiber, $\varepsilon_{s,\text{peak}}$, and the strain in GFRP bar at tension fiber, $\varepsilon_{f,\text{peak}}$, corresponding to peak lateral loads are shown in the table. Table 3 also lists the failure modes corresponding to each specimen.

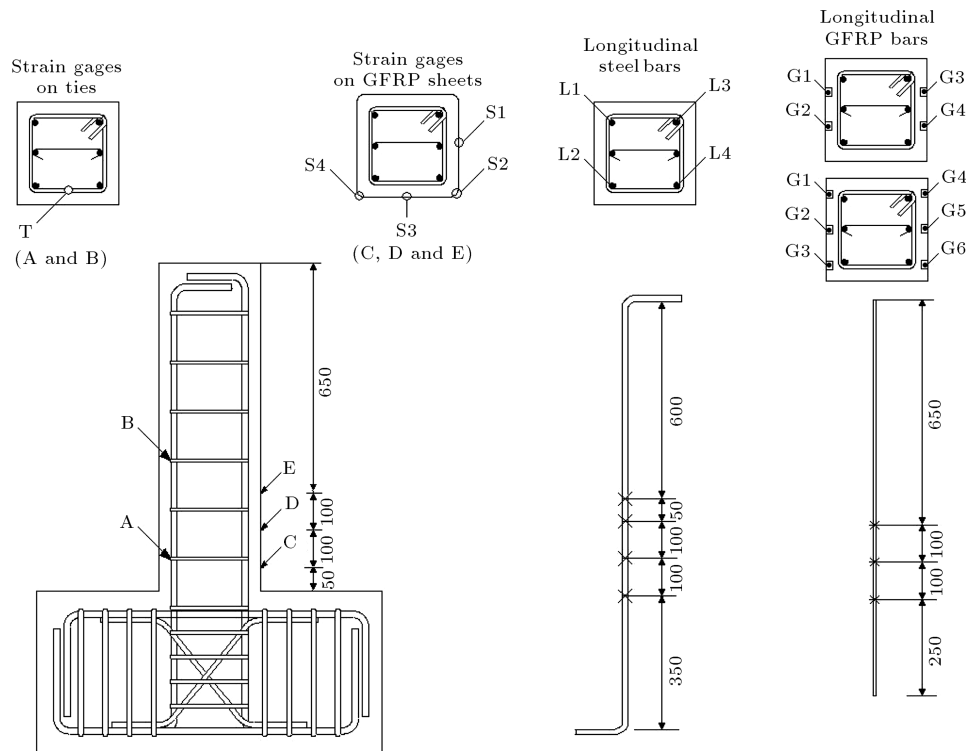


Figure 5. Location of strain gages (all dimensions are in mm).

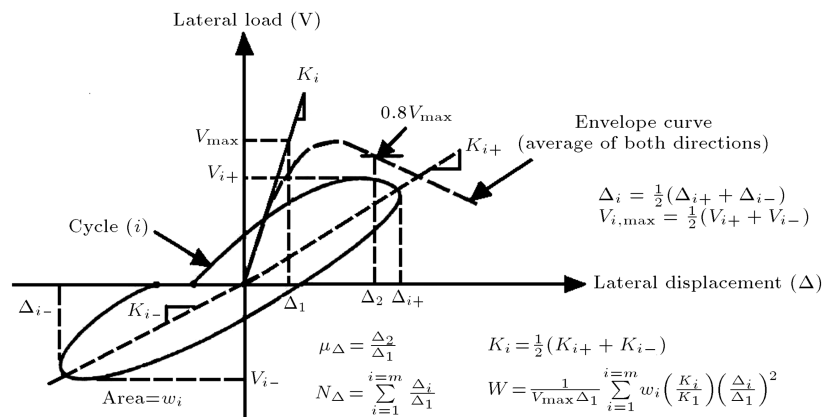


Figure 6. Definition of member ductility parameters suggested by Khoury and Sheikh (1991).

An increase in the axial load from zero to $0.2P_0$ in the unstrengthened specimens caused a considerable reduction in the displacement ductility, μ_{Δ} , from 9.3 to 3.2. Moreover, the cumulative displacement ductility ratio showed a significant reduction from 51 to 34 for $N_{\Delta 80}$, and 22 to 3 for work damage indicator, W_{80} , as a result of an increase in the axial load. The differences were very small for the strengthened specimens.

3.2. Failure modes

At the time the specimens reached to the maximum lateral load, approximately 5 mm wide flexural cracks parallel to the loading direction were observed. These cracks were along with a slight reduction in the flexural

capacity. In the unstrengthened specimens, loss of the flexural strength was regained due to the confining pressure of steel transverse ties and the strain hardening of longitudinal steel bars. Moreover, the loss of flexural strength in the strengthened specimens was regained due to the confining pressure of steel transverse ties, the strain hardening of longitudinal steel bars and the confining pressure of GFRP wraps. In the unstrengthened specimens, the top and bottom cover concrete spalled off along the splitting cracks in the subsequent cycles. The initiation of longitudinal steel bar buckling was observed simultaneous to the spalling of cover concrete in the plastic hinge region. Twenty percent strength drop in the unstrengthened

Table 3. Ductility parameters.

Specimen	V_y^a (kN)	Δ_y (mm)	V_{max} (kN) (%) ^b	μ_Δ (%) ^c	$N_{\Delta 80}$	$N_{\Delta t}$	W_{80}	W_t	$\varepsilon_{c,peak}$ (%)	$\varepsilon_{s,peak}$ (%)	$\varepsilon_{f,peak}$ (%)	Failure mode
C_1	23	7.8	27, (1.5)	9.3, (10)	51	62	22	33	0.21	0.38	-	Concrete-crushing ^d
C_2	51	7.8	59, (1.5)	3.2, (3)	34	62	3	16	0.36	0.5	-	Concrete-crushing ^d
R_1	54	6.4	62, (1.5)	7.7, (7)	53	75	15	35	0.6	1.3	-	No failure
R_2	40	12.2	51, (4)	3.5, (5)	25	40	2	7	0.65	1.5	1.8	Rupture of GFRP bar ^e
R_3	52	10.3	64, (4)	4.9, (7)	33	47	5	12	0.7	1.53	1.85	Rupture of GFRP bar ^e
R_4	69	10.3	84, (4)	5.4, (7)	33	47	4	8	0.75	1.57	1.9	Rupture of GFRP bar ^e
R_5	80	11	101, (4)	4.7, (7)	31	44	2	4	0.72	1.55	1.87	Rupture of GFRP bar ^e

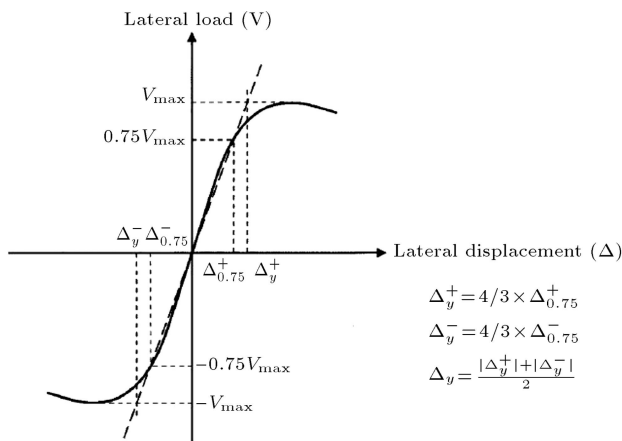
^a: Initiation of yielding in steel bars occurred in cycle with drift ratio 1%;

^b: Drift ratio at maximum lateral load;

^c: Drift ratio demonstrating twenty percent strength drop;

^d: Ductile failure mode, where concrete crushing and buckling of steel bars occurred after yielding of tensile steel bar;

^e: Ductile failure mode, where rupture of GFRP bars occurred after yielding of tensile steel bar.

**Figure 7.** Definition of yield displacement.

specimen C_1 gradually appeared after cycle with drift ratio 7%. Twenty percent strength drop in the unstrengthened specimen C_2 occurred in cycle with drift ratio 3%. In the specimen R_1 strengthened with three layers of GFRP sheets, strength degradation gradually appeared. In this specimen, twenty percent strength drop occurred in cycle with drift ratio 7% without any rupture in GFRP sheets. In the specimens R_2 to R_5 strengthened with longitudinal GFRP bars and GFRP wraps, failure ended up with the rupture of GFRP bars. In the specimens R_3 , R_4 and R_5 , twenty percent strength drop appeared in cycle with drift ratio 7%, whereas in the specimen R_2 , twenty percent strength drop occurred in cycle with drift ratio 5%. Figure 11

shows failure resulted in the rupture of longitudinal GFRP bars in the strengthened specimens R_4 and R_5 .

3.3. Effect of GFRP wraps

GFRP wraps provide effective lateral restraint for longitudinal GFRP bars, prevent the possible instability of longitudinal steel bars under compression and control the spalling of cover concrete. In this study, the experimental results in the strengthened specimens showed noticeable displacement ductility without considerable contribution to the flexural strength up to 5%. The following results are also concluded:

- The confinement effect of the specimen C_2 by three layers of GFRP sheets showed 140% increase in member ductility ratio, μ_Δ , in the specimen R_1 .
- The compressive strain at the extreme compression fiber at peak load, $\varepsilon_{c,peak}$, in the strengthened specimen R_1 was shown to be on average 70% higher than that of the unstrengthened specimen C_2 . Moreover, $\varepsilon_{c,peak}$, in the strengthened specimens R_2 to R_5 was shown to be on average from 80% to 110% higher than that of the unstrengthened specimen C_2 , respectively. Consequently, GFRP wraps increase the ultimate strain of concrete columns.

3.4. Stub effect

It is known that the maximum moment in the column occurs at the column-stub interface. However, failure in column is initiated at a section away from the face of the stub. The shift in the location of the critical section toward the neighboring sections, provided by

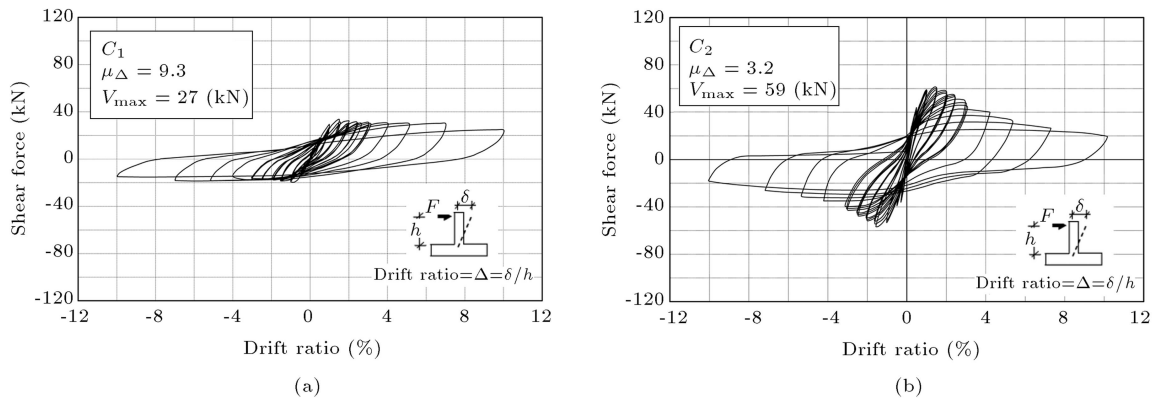


Figure 8. Shear force vs. drift ratio curves in the unstrengthened specimens; a) C_1 ; and b) C_2 .

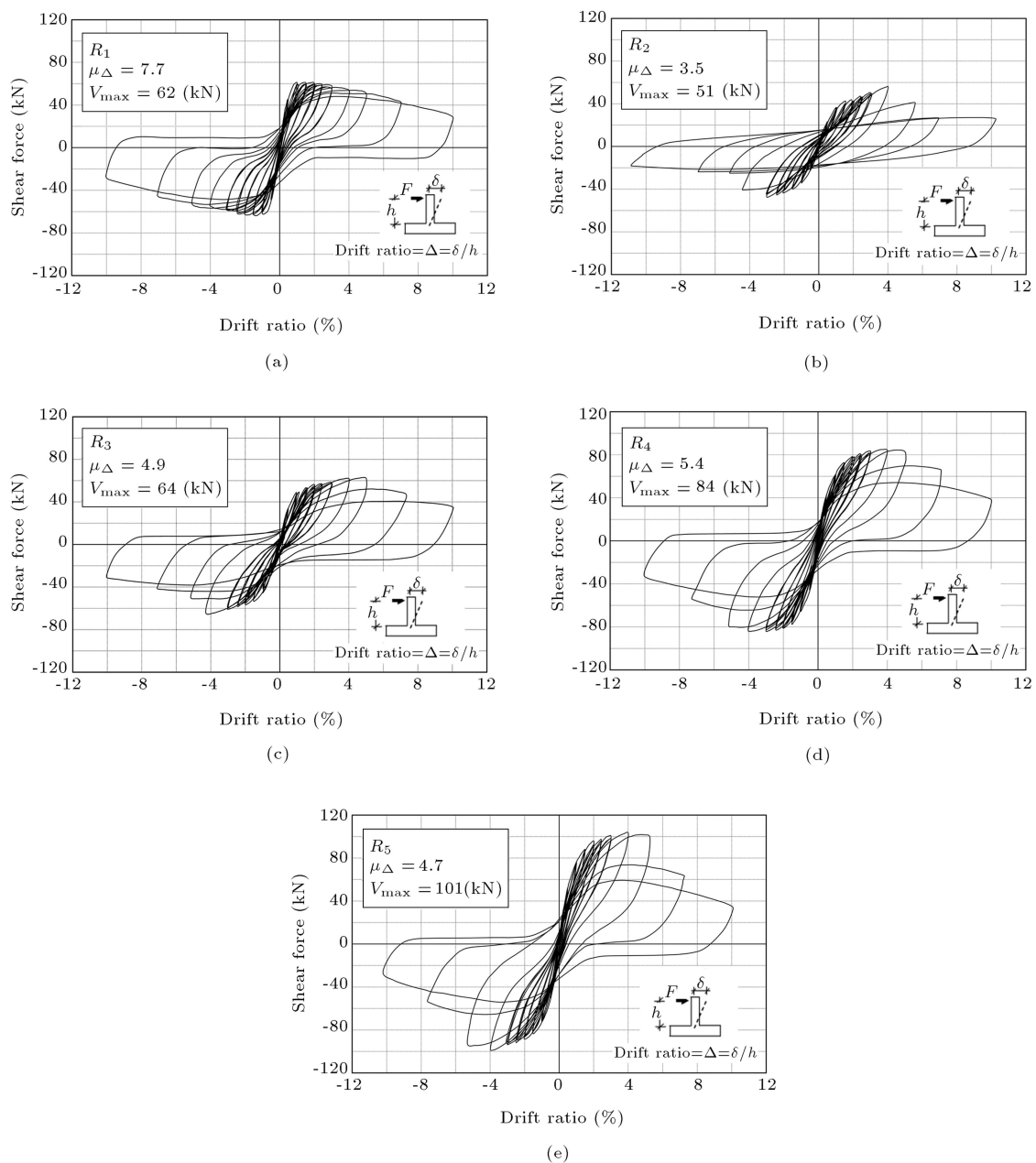


Figure 9. Shear force vs. drift ratio curves in the strengthened specimens; a) R_1 ; b) R_2 ; c) R_3 ; d) R_4 and e) R_5 .

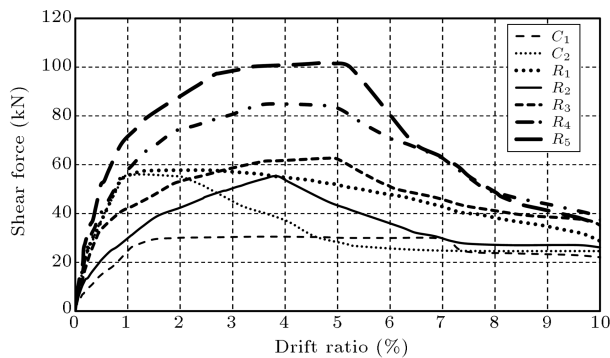


Figure 10. Envelope curves of shear force vs. drift ratio in the unstrengthened and strengthened specimens.



Figure 11. Failure as a result of GFRP bar rupturing in the strengthened columns: a) R_4 ; and b) R_5 .



Figure 12. Stub effect; sections within a distance of approximately 50 mm from the stub remained nearly undamaged.

the confinement effect of concrete stub, causes delay in spreading of cracks in concrete, and reduces the tendency of lateral expansion. Consequently, due to the increased moment capacity of the critical section, failure shifts to a nearby section. This effect has been observed in the previous experimental researches [27–31]. Figure 12 shows the most damaged regions of the columns in the unstrengthened specimens. In these

specimens, due to the additional confinement provided by the stub, sections within a distance of approximately 50 mm from the stub remained nearly undamaged.

3.5. Effect of longitudinal GFRP bars

The previous researches have revealed that longitudinal GFRP bars can significantly enhance the flexural strength of the RC columns [23–24]. In this study, by reinforcing the unstrengthened specimen C_2 with 4 and 6 longitudinal NSM-GFRP bars ($\rho_{NSM} = 0.5\%$ and 0.75%), under axial load level, $0.2P_0$, the maximum lateral load was upgraded by 40% in the specimen R_4 and 70% in the specimen R_5 , respectively. Furthermore, strengthening the specimen C_1 without axial load and with 4 longitudinal NSM-GFRP bars resulted in 90% increase in the maximum lateral load in the specimen R_2 . These upgrading levels in the flexural strength of the strengthened columns occurred as a result of adding longitudinal GFRP bars to the unstrengthened specimens C_1 and C_2 in Near-Surface Mounted technique.

4. Conclusions

To evaluate the performance and capacity of reinforced concrete columns, strengthened with longitudinal NSM-GFRP bars and GFRP wraps, seven half-scale square RC columns were tested under constant axial and cyclic lateral loads. The following conclusions are derived based on the experimental results:

- The confinement effect with three layers of GFRP sheets provides noticeable displacement ductility without considerable contribution to flexural strength (maximum 5% increase in flexural strength). Additionally, GFRP wraps provide effective lateral restraint for longitudinal steel, and GFRP bars prevent the possible instability of longitudinal bars under compression and control the spalling of cover concrete.
- GFRP wraps increase the strain capacity in compressive concrete of the strengthened columns from 70% to 110%, with respect to the strain capacity in compressive concrete of the unstrengthened columns. Moreover, confinement with three layers of GFRP sheets increases the member ductility ratio, μ_Δ , up to 140% in the strengthened specimen R_1 .
- The failure of the strengthened specimens (R_2 to R_5), due to the rupture of GFRP bars, indicates that full flexural capacity develops at the base level of the columns. In addition, this failure demonstrates that significant bond strength is provided by anchoring GFRP bars with embedment length of approximately 250 mm into the stub.
- The strengthening of the specimens with GFRP bars shows a significant increase in flexural strength of

the RC columns. For the specimens with axial load level, $0.2P_0$, by increasing NSM-GFRP bar reinforcement ratios from $\rho_{NSM} = 0.5\%$ to 0.75% , the flexural strength was upgraded from 40% to 70%. Finally, for the specimens without axial load by retrofitting the unstrengthened specimen with four GFRP bars, $\rho_{NSM} = 0.5\%$, the flexural strength was upgraded up to 90%. These upgrading levels of the strengthened specimens reliably confirm the efficiency of GFRP bars in Near-Surface Mounted technique to enhance the flexural strength of RC columns.

Acknowledgements

The authors wish to acknowledge the financial support, provided by the "Building and Housing Research Center (BHRC) of Iran". The authors also extend their gratitude to Dr. S.M. Fatemi Aghda, President of Building and Housing Research Center and for his helps in conducting experimental tests. Also, the assistance of laboratory staff, including Alizadeh and Nooshabadi, is greatly acknowledged.

References

1. Balaguru, P., Nanni, A. and Giancaspro, J., *FRP Composites for Reinforced and Prestressed Concrete Structures*, Taylor & Francis, New York, USA (2009).
2. Hollaway, L. and Teng, J., *Strengthening and Rehabilitation of Civil Infrastructure Using Fiber Reinforced Polymer (FRP) Composites*, Woodhead Publishing, UK (2008).
3. Teng, J.G., Chen, J.F., Smith, S.T. and Lam, L., *FRP-Strengthened RC Structures*, John Wiley & Sons, Ltd, UK (2002).
4. Ghosh, K. and Sheikh, S. "Seismic upgrade with carbon fiber reinforced polymer of columns containing lap-spliced reinforcing bars", *ACI Structural J.*, **104**(2), pp. 227-236 (2007).
5. ACI 440.2R "Guide for the design and construction of externally bonded FRP systems for strengthening concrete structures", American Institute, Farmington Hills, Michigan, USA (2008).
6. Eslami, A. and Ronagh, H.R. "Effect of FRP wrapping in seismic performance of RC buildings with and without special detailing - A case study", *Composites. Part B: Engineering*, **45**, pp. 1265-1274 (2013).
7. Ronagh, H.R. and Eslami, A. "Flexural retrofitting of RC buildings using GFRP/CFRP - A comparative study", *Composites Part B: Engineering*, **46**, pp. 188-196 (2013).
8. Mahini, S.S. and Ronagh, H.R. "Strength and ductility of FRP web-bonded RC beams for the assessment of reinforced beam-column joints", *Composite Structures*, **92**, pp. 1325-1332 (2010).
9. Mahini, S.S. and Ronagh, H.R. "Web-bonded FRPs for relocation of plastic hinges away from the column face in exterior RC joints", *Composite Structures*, **93**, pp. 2460-2472 (2011).
10. Dalalbashi, A., Eslami, A. and Ronagh, H.R. "Plastic hinge relocation in RC joints as an alternative method of retrofitting using FRP", *Composite Structures*, **94**, pp. 2433-2439 (2012).
11. Asplund, S.O. "Strengthening bridge slabs with grouted reinforcement", *J. the American Concrete Ins.*, **20**(6), pp. 397-406 (1949).
12. Barros, J. and Fortes, A. "Flexural strengthening of concrete beams with CFRP laminates bonded into slits", *Cement and Concrete Composites*, **27**(7), pp. 471-480 (2005).
13. Parretti, R. and Nanni, A. "Strengthening of RC members using near-surface mounted FRP composites: Design overview", *Advances in Structural Eng.*, **7**(5), pp. 1-16 (2004).
14. Tinazzi, D. and Nanni, A. "Assessment of technologies of masonry retrofitting with FRP", *CIES 00-18, Center for Infrastructure Engrg. Studies*, University of Missouri-Rolla (2000).
15. De Lorenzis, L. and Nanni, A. "Strengthening of RC structures with near surface mounted FRP rods", *CIES 99-10, Center for Infrastructure Engrg. Studies*, University of Missouri Rolla (1999).
16. De Lorenzis, L. and Nanni, A. "Characterization of FRP rods as near surface mounted reinforcement", *J. of Composites for Construction ASCE*, **5**(2), pp. 114-121 (2001).
17. De Lorenzis, L. and Nanni, A. "Shear strengthening of reinforced concrete beams with near surface mounted fiber reinforced polymer rods", *ACI Structural J.*, **98**(1), pp. 60-68 (2001).
18. Yost, J., Gross, S., Dinehart, D. and Mildenberg, J. "Flexural behavior of concrete beams strengthened with near surface mounted CFRP strips", *ACI Structural J.*, **104**(4), pp. 430-437 (2007).
19. Barros, J., Ferreira, D., Fortes, A. and Dias, S. "Assessing the effectiveness of embedding CFRP laminates in the near surface for structural strengthening", *Construction and Building Materials*, **20**(7), pp. 478-491 (2006).
20. Carolin, A., Taljsten, B. and Hejll, A. "Concrete beams exposed to live loading during carbon fiber reinforced polymer strengthening", *J. of Composites for Construction ASCE*, **9**(2), pp. 178-188 (2005).
21. El-Hacha, R. and Rizkalla, S. "Near-Surface-mounted fiber-reinforced polymer reinforcements for flexural strengthening of concrete structures", *ACI Structural J.*, **101**(5), pp. 717-726 (2004).
22. Nanni, A., Alkhrdaji, T., Barker, M., Chen, G., Mayo, R. and Yang, X. "Overview of testing to failure program of a highway bridge strengthened with FRP composites", *Proceedings of 4th Int. Symposium on Non-Metallic (FRP) Reinforcement for Concrete Structures*, Mich., USA, pp. 69-75 (1999).

23. Alkhrdaji, T., Nanni, A. and Chen, G. "Destructive and non-destructive testing of bridge J857 Phelps County, Missouri", CIES 99-08C, Center for Infrastructure Engrg. University of Missouri Rolla (1999).
24. Bournas, D. and Triantafillou, T. "Flexural strengthening of RC columns with NSM FRP or stainless steel", *ACI Structural J.*, **106**(4), pp. 495-505 (2009).
25. Priestley, M., Seible, F. and Calvi, G.M., *Seismic Design and Retrofit of Bridges*, John Wiley & Sons, Inc., New York, USA (1996).
26. Priestley, M.J.N., Calvi, G.M. and Kowalsky, M.J., *Displacement Based Seismic Design of Structures*, IUSS PRESS, Pavia, Italy (2007).
27. Khoury, S.S. and Sheikh, S.A. "Behavior of normal and high strength confined concrete columns with and without stubs", Research Report No. UHCEE 91-04, University of Houston, Tex (1991).
28. Bayrak, O. and Sheikh, S.A. "Confinement reinforcement design considerations for ductile HSC columns", *J. of Structural Engrg. ASCE*, **124**(9), pp. 999-1010 (1998).
29. Legeron, F. and Paultre, P. "Behavior of high-strength concrete columns under cyclic flexure and constant axial load", *ACI Structural J.*, **97**(4), pp. 591-601 (2000).
30. Park, R., Priestley, M.J.N. and Gill, W.D. "Ductility of square confined concrete columns", *J. of Structural Division ASCE*, **108**(ST4), pp. 929-950 (1982).
31. Sheikh, S.A. and Khoury, S. "Confined concrete columns with stubs", *ACI Structural J.*, **90**(4), pp. 414-431 (1993).

Biographies

Nima Dayhim is a PhD degree candidate in the Department of Civil Engineering at Iran University of Science and Technology, Tehran, Iran, where he also received his MS degree. His research interests include: seismic rehabilitation of structures, seismic pathology,

evaluating the seismic behavior of reinforced concrete structures, earthquake resistance design of structures and bridges, fracture mechanics, structural mechanics & stability and also numerical and functional analysis and approximation.

Ahmad Nicknam, PhD, is Assistant Professor in the Department of Civil Engineering at Iran University of Science and Technology, Tehran, Iran. He has published numerous papers in international journals and conferences as authored/co-authored in the fields of earthquake simulation at near and far source sites including directivity effects, nonlinear dynamic analysis and performance evaluation of structures, retrofitting structures, deterministic and probabilistic USHA.

Mohammad Ali Barkhordari, PhD, is Associate Professor in the Department of Civil Engineering at Iran University of Science and Technology, Tehran, Iran. He received his PhD degree from Michigan State University. His research interests include: structural stability and seismic design and retrofitting of structures.

Abdollah Hosseini, PhD, is Assistant Professor in the Department of Civil Engineering at Tehran University, Tehran, Iran. He received his PhD degree from Sharif University of Technology. His research interests include: seismic design and rehabilitation of structures.

Shahab Mehdizad, MS, graduated in Structure Engineering at Sharif University of Technology, Tehran, Iran. He received his BS degree from Iran University of Science and Technology. He has published numerous papers in international journals and conferences as authored/co-authored in the fields of seismic retrofit of reinforced concrete structures. At present, he is the managing director of the Payon retrofitting company.